Journal of Materials Chemistry B

ROYAL SOCIETY OF CHEMISTRY

PAPER

View Article Online
View Journal | View Issue

Cite this: J. Mater. Chem. B, 2024, 12, 8647

Broad-spectrum degradation of fluoroquinolone antibiotics by Hemin-His-Fe nanozymes with peroxidase-like activity†

Xin Geng,[a] Kexu Song,[a] Qingying Hu,[a] Yue Yin,[b] Haisong Li,*[b] Xiyun Yan*[acd] and Bing Jiang *[ac]

Received 9th March 2024,
Accepted 15th July 2024

DOI: 10.1039/d4tb00508b

rsc.li/materials-b

Fluoroquinolones are a widely used class of antibiotics, with a large variety, which are frequently monitored in the aqueous environment, threatening ecological and human health. To date, effective degradation of fluoroquinolone antibiotics remains a major challenge. Focused on the broad-spectrum degradation of fluoroquinolone antibiotics, a novel biomimetic peroxidase nanozyme named Hemin-His-Fe (HHF)-peroxidase nanozyme was synthesized through a green and rapid "one-pot" method involving hemin, Fmoc-L-His and Fe^{2+} as precursors. After systematic optimization of the reaction conditions, fluoroquinolone antibiotics can be degraded by the HHF-peroxidase nanozyme when supplemented with H_2O_2 in acidic environments. Through validation and analysis, it was proved that the generated strong oxidative hydroxyl radicals are the main active species in the degradation process. In addition, it was verified that this method shows great universal applicability in real water samples.

Introduction

Excessive preparation and use of antibiotics has resulted in a significant influx of antibiotic pollutants into aqueous ecosystems, exacerbating the problem of aqueous environment pollution.[1–3] Among them, fluoroquinolones stand out as widely utilized agents for the treatment of bacterial infections in humans and animals.[4–6] Zhang *et al.* estimated that China alone consumed approximately 27 300 tons of fluoroquinolones in 2013, accounting for 17% of total antibiotic usage.[7] However, due to their inherent stability and poor biodegradability, they are degraded with difficulty in the environment. Consequently, unutilized fluoroquinolones are discharged into surface water and eventually reach drinking water sources and near-shore seawater, and in turn accumulate in ecosystems. This accumulation poses a triple threat: bacterial resistance, human health risks, and ecosystem disruption.[8–10] Therefore, the development of effective methods to degrade residual fluoroquinolone antibiotics in aqueous environments is important for environmental protection.

The variety of fluoroquinolone antibiotics is extensive, typically including norfloxacin, ofloxacin, enrofloxacin, ciprofloxacin, *etc.*,[11] and it is necessary to develop degradation methods with a broad-spectrum degradation capability. Various methods and strategies have been explored for fluoroquinolone antibiotic degradation,[12–15] where advanced oxidation techniques based on nanomaterials are predominantly employed.[16,17] However, many methods within this category depend on additional energy sources, such as light, ultrasound, or electricity, and often involve

[a] Nanozyme Laboratory in Zhongyuan, School of Basic Medical Sciences, Zhengzhou University, Zhengzhou, Henan, 450001, China. E-mail: yanxy@ibp.ac.cn, jiangbing@zzu.edu.cn
[b] College of Ecology and Environment, Zhengzhou University, Zhengzhou 450001, China. E-mail: lhs@zzu.edu.cn
[c] Nanozyme Laboratory in Zhongyuan, Henan Academy of Innovations in Medical Science, Zhengzhou, Henan, 451163, China
[d] CAS Engineering Laboratory for Nanozyme, Key Laboratory of Biomacromolecules, Institute of Biophysics, Chinese Academy of Sciences, Beijing 100101, China

† Electronic supplementary information (ESI) available. See DOI: https://doi.org/10.1039/d4tb00508b

Bing Jiang

Bing Jiang received his PhD degree in cell biology from the Institute of Biophysics, Chinese Academy of Sciences in 2019. Then he worked at Nanozyme Laboratory in Zhongyuan, School of Basic Medical Sciences, Zhengzhou University and was promoted to associate professor in 2021. He focuses on the medical research of nanozymes, particularly in the construction and application of efficient nanozyme systems from structural design to cascade catalysis.

complex material preparation processes. Additionally, most of them tend to focus solely on the degradation effects of a single fluoroquinolone antibiotic.[18–25] Consequently, there is a pressing need to explore a simpler and more energy-efficient method with broad-spectrum degradation capability for the effective degradation of fluoroquinolone antibiotics in aqueous environments.

Nanozymes, as a new generation of artificial enzymes, offer a promising solution to this challenge.[26] Nanozymes are alternatives to natural enzymes due to their advantages of low cost, high stability, ease of scalable production and multifunctionality. They have been applied in a variety of fields such as diagnosis of diseases, antibacterials, cancer therapy, biosensing, and so on.[27–34] Among them, peroxidase nanozymes, a class of classical redox nanozymes, possess the ability to catalyze H_2O_2 to produce hydroxyl radicals ($^{\bullet}OH$) with strong oxidative activity.[35,36] This oxidative activity represents an efficient approach to degrade pollutants without the inhibitory effects associated with biological methods and without the requirement of additional energy. Recent studies have demonstrated the effectiveness of peroxidase nanozymes in removing organic compounds, such as phenol, aniline, dyes, pesticides, and microplastics, from wastewater.[37–46] Consequently, the development of easily prepared peroxidase nanozymes offers a promising avenue for achieving broad-spectrum degradation of fluoroquinolone antibiotics in aqueous environments.

In this work, we synthesized a Hemin-His-Fe (HHF)-peroxidase nanozyme by mimicking the structural features of natural peroxidases. The synthesis was accomplished through a green and rapid "one-pot" method involving hemin, Fmoc-L-His and Fe^{2+} as precursors. The HHF-peroxidase nanozyme demonstrated successful fluoroquinolone antibiotic degradation based on peroxidase-like activity (Scheme 1). By systematically investigating various reaction conditions, including the concentration, time, and pH, we identified the optimal conditions for norfloxacin degradation. Our HHF-based method has been demonstrated to achieve effective qualitative degradation of norfloxacin. Furthermore, the mechanistic study revealed that $^{\bullet}OH$ played a pivotal role in norfloxacin degradation. Importantly, our findings extended beyond norfloxacin, as the HHF-peroxidase nanozyme exhibited the ability to degrade other fluoroquinolone antibiotics, including ofloxacin, enrofloxacin and ciprofloxacin. Finally, we successfully realized the degradation of fluoroquinolone antibiotics in real water samples using HHF-peroxidase nanozyme.

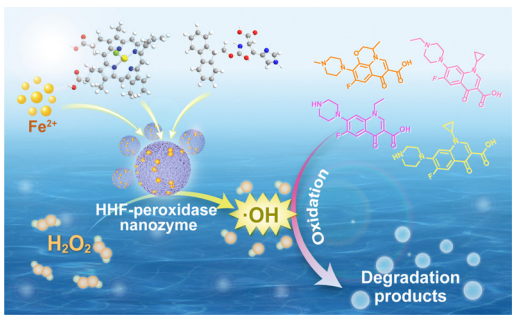

Scheme 1 Hemin-His-Fe (HHF)-peroxidase nanozyme for fluoroquinolone antibiotics degradation.

Materials and instrumentation

Materials

Norfloxacin, ofloxacin, enrofloxacin and ciprofloxacin (98%) were from Saan Chemical Technology Co. Ltd (Shanghai, China). Fmoc-L-histidine (Fmoc-L-His, 97%), hemin (98%) and coumarin (99%) were purchased from Shanghai Macklin Biochemical Technology Co., Ltd (China). All reagents were used without further purification.

Instrumentation

The UV-vis spectrum and fluorescence intensities were obtained by the Spark microplate reader (Tecan, Austria). Talos L120CG2 (Thermo Fisher Scientific, Czech) was used to capture the transmission electron microscopy (TEM) image of the HHF-peroxidase nanozyme. The Fourier transform infrared (FTIR) spectrum was performed on an IRTracer-100 FTIR spectrophotometer (Shimadzu, Japan). The X-ray photoelectron spectroscopy (XPS) of HHF-peroxidase nanozyme was obtained on a Thermo Scientific K-Alpha.

Experimental methods

Synthesis of the HHF-peroxidase nanozyme

The HHF-peroxidase nanozyme was synthesized in "one-pot" through stirring at room temperature. First, hemin (2.5 mM) and Fmoc-L-His (5 mM) dissolved with DMSO are added into H_2O, and $FeCl_2{\cdot}4H_2O$ (5 mM) was added under constant magnetic stirring. Next, NaOH (1 M) was added to the mixture to adjust the pH to around 7.0. After stirring for 10 min, the mixture was continuously sonicated for 10 min. Then, dialysis was used to remove the unreacted small precursors for 24 h. The black precipitates were collected by centrifugation at 12 000 rpm for 10 min. Then, the precipitates were dispersed with H_2O and sonicated to make them well dispersed. Finally, the products were collected through vacuum freeze-drying technology.

Peroxidase-like activity assay

The peroxidase-like activity of the HHF-peroxidase nanozyme was determined by the substrate of TMB in the presence of H_2O_2. First, the HHF-peroxidase nanozyme (0.02 mg mL^{-1}) was added into the HAc-NaAc buffer (0.2 M, pH 4.0) containing TMB (0.2 mg mL^{-1}) and H_2O_2 (5 mM). After 10 min, the UV-vis absorbance spectrum of the oxidized TMB was collected. The HHF-peroxidase nanozyme concentration dependence of peroxidase-like activity was investigated by employing different concentrations of HHF-peroxidase nanozyme (0.001–0.02 mg mL^{-1}) in the mixture. The H_2O_2 dependence of the peroxidase-like activity was carried out through employing different concentrations of H_2O_2 (0–5 mM) in the mixture. And the pH dependence of the peroxidase-like activity was investigated by adding HHF-peroxidase nanozyme in different pH buffers.

$^{\bullet}OH$ detection

Coumarin was used as a fluorescence probe to determine the produced $^{\bullet}OH$. HHF-peroxidase nanozyme (0.1 mg mL^{-1}) and

H_2O_2 (15 mM) were added into coumarin solution (1 mM, pH 4). After 4 h, the fluorescence intensities were recorded at 460 nm, where the excitation wavelength is 345 nm. For the assay of pH dependence of $^{\bullet}OH$ production, HHF-peroxidase nanozyme and H_2O_2 were added into coumarin solutions with different pHs. Moreover, isopropanol (20 mM) was added to the mixture to inhibit the production of $^{\bullet}OH$.

Fluoroquinolone antibiotics degradation

Norfloxacin was well dispersed in H_2O by ultrasonication to formulate a mixture with a concentration of 1 mg mL^{-1}. The HHF-peroxidase nanozyme (0.1 mg mL^{-1}) was added to a mixture containing norfloxacin (20 μg mL^{-1}), H_2O_2 (15 mM), and H_2O (pH 4). After 4 h, the absorbance of norfloxacin at 276 nm was measured, and the absorbance at 800 nm was used as a control. Degradation tests for ofloxacin, enrofloxacin and ciprofloxacin were performed as in the above steps.

Fluoroquinolone antibiotics degradation in real water samples

The real water samples were first filtered through a 0.22 μm filter film to remove the large substances and adjust the pH to 4 using HCl. Then, HHF-peroxidase nanozyme (0.1 mg mL^{-1}) and H_2O_2 (15 mM) were added to the mixture containing norfloxacin (20 μg mL^{-1}) and different real samples (pH 4). After 4 h, the absorbance of fluoroquinolone antibiotics was measured.

Results and discussion

Synthesis and characterization of the HHF-peroxidase nanozyme

The active site structure of natural enzymes can effectively regulate the type and activity of catalytic reactions.[47–49] Therefore, it is feasible to prepare nanozymes with peroxidase-like activity by mimicking the active site of a natural peroxidase. In this work, nanozymes with excellent peroxidase-like activity were prepared by mimicking the structural features of horseradish peroxidase (HRP) through designing and selecting suitable precursors. Hemin, an iron porphyrin compound, is the active center structure of many natural enzymes (*e.g.*, HRP), and the iron ions in the center can transfer electrons, which in turn enables it to perform catalytic activities.[50] Amino acids are the basic units of natural enzymes. Among them, histidine (His) has an important role in natural peroxidases, which can usually facilitate enzyme action by assisting the localization of H_2O_2 to the active center through hydrogen bonds.[51] Therefore, by introducing the functional structural units of hemin and His, nanomaterials can be effectively endowed with peroxidase-like activity.

Moving on to the method of synthesis, self-assembly is a method of spontaneous organization or aggregation of molecules into stable structures by means of non-covalent bonding interactions. In order to synthesize peroxidase nanozymes in a fast and green way, herein, we prepared a novel biomimetic peroxidase nanozyme named Hemin-His-Fe (HHF)-peroxidase nanozyme by self-assembly using hemin, Fmoc-L-His and Fe^{2+} as precursors in "one-pot" at room temperature and pressure (Fig. 1(a)). Among them, hemin and Fmoc groups can be aggregated by intermolecular π–π conjugation; hydrogen bonds can be formed between the carboxyl group of hemin and the carboxyl/amide groups of Fmoc-L-His, which is the crucial key to self-assembly. The addition of Fe^{2+} can further promote the process of self-assembly, which allows coordination with the carboxyl and amide groups, and also facilitates electron transfer to perform peroxidase-like activity (Fig. S1, ESI†).

Having established the synthesis process, we then moved on to characterize the HHF-peroxidase nanozyme. Transmission electron microscopy (TEM) images revealed that the HHF-peroxidase nanozyme obtained by self-assembly presented a generally spherical-like morphology with some degree of aggregation, and their average size is approximately 157.2 nm (Fig. 1(b) and Fig. S2, ESI†). The DLS data revealed an average hydrated particle size of 167.4 nm in an aqueous environment (Fig. 1(c)). X-ray photoelectron spectroscopy (XPS) results were used to analyze the surface compositions of the HHF-peroxidase nanozyme. The XPS results showed that the HHF nanozyme was composed of C, N, O, Cl, and Fe. The high-resolution C 1s spectrum can be fitted to three peaks, which are C═O/C═N (288.8 eV), C–N/C–O (285.6 eV) and C–C/C═C (284.7 eV) (Fig. 1(d)). The high-resolution N 1s spectrum can be fitted to three peaks of 398.5, 399.9, and 400.8 eV, corresponding to N–H, Fe–N, and pyrrolic N (Fig. 1(e)). As shown in Fig. 1(f), the high-resolution O 1s spectrum featured three peaks centered at 530.7 eV, 531.7 eV and 532.9 eV, typical to O–H, C═O and C–O. The Cl 2p XPS spectrum can be fitted to two peaks, which are Cl $2p_{3/2}$ (198.0 eV) and Cl $2p_{1/2}$ (199.1 eV) (Fig. 1(g)). These results indicate that the HHF-peroxidase nanozyme retained the functional groups of the precursors on their surfaces. As shown in Fig. 1(h), the high-resolution Fe 2p spectrum can be clearly divided into four peaks, which are Fe^{2+} $2p_{3/2}$ (710.8 eV), Fe^{3+} $2p_{3/2}$ (714.0 eV), Fe^{2+} $2p_{1/2}$ (724.4 eV) and Fe^{3+} $2p_{1/2}$ (727.4 eV), implying that the presence of iron in the two variegated forms would be favorable for the performance of the peroxidase-like activity. The HHF-peroxidase nanozyme was further scrutinized by Fourier transform-infrared (FTIR) spectroscopy, and similar to the XPS results, where the surface retained the precursor functional groups. The absorption peaks at 3421, 2920, 1701, 1084, 1620 and 1319 cm^{-1} corresponded to the stretching vibration of O–H/N–H, C–H, C═O, C–O–H, C═C/C═N and C–N (Fig. S3, ESI†). The above results sufficiently demonstrated that HHF-peroxidase nanozyme with functional structures of natural peroxidase active centers were successfully prepared by self-assembly without destroying the precursor structures of hemin, Fmoc-L-His and Fe^{2+}.

Peroxidase-like activity of the HHF-peroxidase nanozyme

The peroxidase-like activity test of the HHF-peroxidase nanozyme was carried out using the colorimetric method with 3,3′,5,5′-tetramethylbenzidine (TMB) as the substrate in the presence of H_2O_2 (Fig. 2(a)). In the presence of peroxidase and H_2O_2, TMB can be oxidized to oxTMB, changing the color from colorless to blue. Under acidic conditions (pH 4.0), no significant changes were observed in the UV-vis absorption spectra when only H_2O_2 or HHF-peroxidase nanozyme existed.

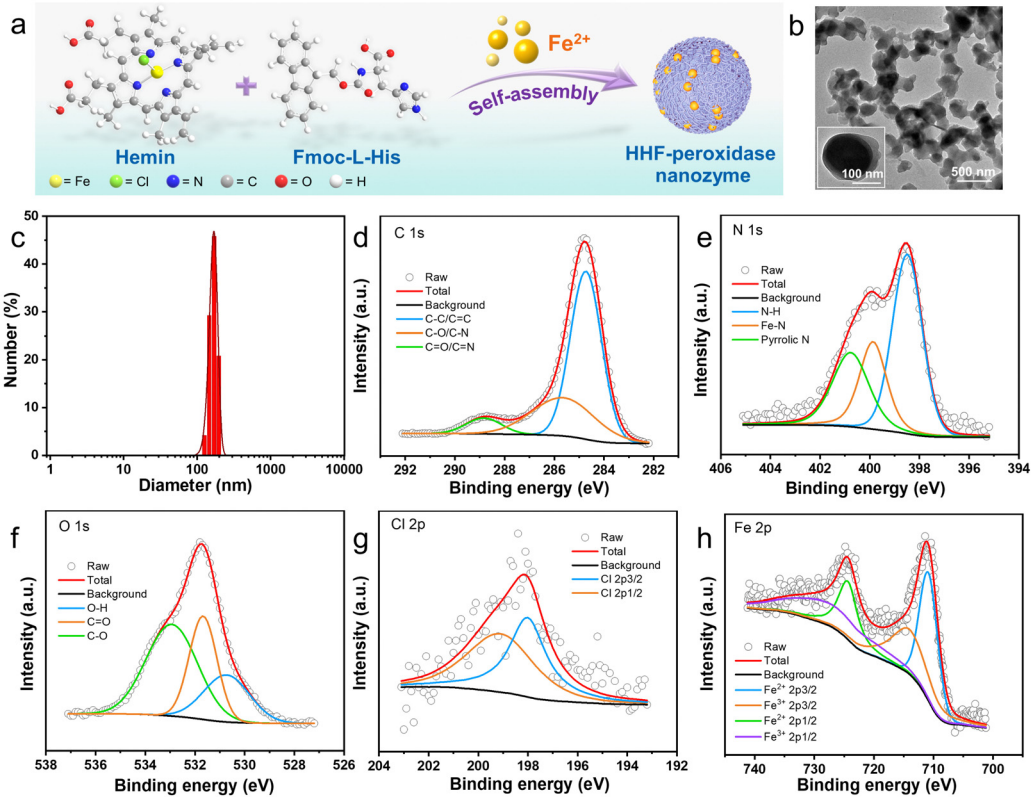

Fig. 1 (a) The synthesis process of HHF-peroxidase nanozyme. (b) TEM images and (c) DLS analysis of HHF-peroxidase nanozyme. (d) C 1s, (e) N 1s, (f) O 1s, (g) Cl 2p and (h) Fe 2p XPS spectrum of the HHF-peroxidase nanozyme.

However, when both coexisted, the absorption peak at 652 nm significantly increased (Fig. 2(b) and (c)). This shows that the HHF-peroxidase nanozyme, formed by self-assembly, possesses the catalytic activity of natural peroxidases. The peroxidase-like activity of HHF varied with H_2O_2 concentration and HHF concentration (Fig. 2(d) and Fig. S4, ESI†). The absorbance of oxidized TMB also increased with HHF or H_2O_2 concentration. Like natural peroxidases, the optimal pH conditions for HHF-peroxidase nanozyme activity are acidic, whereas its activity reduces in alkaline conditions (Fig. 2(e) and (f)). This result

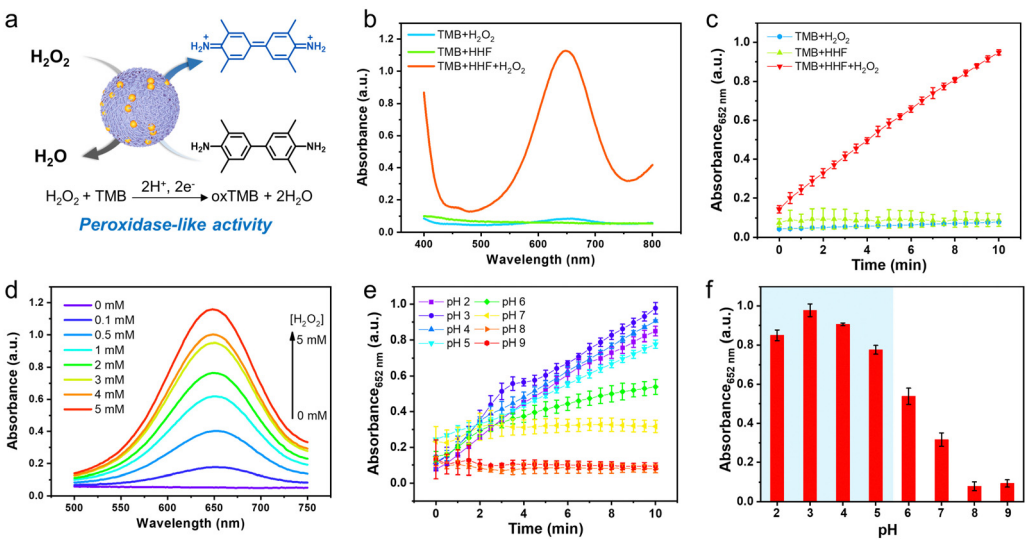

Fig. 2 (a) Schematic illustration of the peroxidase-like activity of the HHF-peroxidase nanozyme. (b) UV-vis absorbance spectra of TMB in different reaction systems. (c) Time-dependent peroxidase-like activity. (d) Peroxidase-like activity of the HHF-peroxidase nanozyme with different concentrations of H_2O_2. (e) and (f) Peroxidase-like activity of the HHF-peroxidase nanozyme at different pH conditions.

indicates that norfloxacin can be degraded in an acidic environment based on the peroxidase-like activity of HHF. Moreover, we performed enzymatic kinetics analyses of the HHF-peroxidase nanozyme and observed typical Michaelis–Menten curves for the substrates H_2O_2 and TMB (Fig. S5, ESI†). The Michaelis–Menten constants (K_m) were determined to be 1.151 mM for H_2O_2 and 0.022 mg mL^{-1} for TMB. Correspondingly, the maximal initial rates (V_{max}) were 1.083 μM min^{-1} for H_2O_2 and 0.879 μM min^{-1} for TMB.

Broad-spectrum degradation of fluoroquinolone antibiotics

Fluoroquinolone antibiotics are a class of pharmaceuticals extensively employed in clinical settings, containing a variety of species. To explore the degradation ability of HHF, norfloxacin was first chosen as an example to carry out the related experiments. Degradation of norfloxacin by HHF involves simply adding HHF-peroxidase nanozyme and H_2O_2 to an acidic solution containing norfloxacin for a certain duration (Fig. 3(a)). UV-vis absorption spectra at 276 nm showed a decrease in norfloxacin peak intensity when both HHF and H_2O_2 were present (Fig. 3(b)). However, in the absence of H_2O_2, norfloxacin degradation by HHF was minimal (Fig. S6, ESI†). Next, the optimal conditions for the degradation of norfloxacin using HHF were explored by adjusting the reaction conditions. Fig. 3(c) and (d) illustrate that as time progresses, norfloxacin's absorbance consistently diminishes, signifying an augmented degradation rate. At the 4-hour mark, approximately 65% of norfloxacin was eradicated. Notably, the degradation trajectory manifested a dependence on H_2O_2 concentration. As the H_2O_2 concentration escalated, a commensurate decline in norfloxacin's absorbance was observed, indicating an enhanced degradation efficiency. Beyond a concentration of 15 mM, no discernible alteration in degradation rate was observed (Fig. 3(e) and (f)), leading to the selection of 15 mM as the optimal H_2O_2 concentration. Furthermore, the influence of pH on norfloxacin degradation facilitated by HHF-peroxidase nanozyme was assessed. Fig. 3(g) and (h) indicates that the degradation mechanism is pH-responsive. In acidic milieu, there was a decline in norfloxacin absorbance, whereas an ascent was observed with elevated pH levels. This suggests that the HHF-peroxidase nanozyme is predominantly efficacious in acidic environments, aligning with HHF's inherent propensity to display peroxidase-like attributes exclusively under such conditions.

In order to further investigate the broad-spectrum of HHF for degrading other fluoroquinolone antibiotics, ofloxacin, enrofloxacin and ciprofloxacin were selected for degradation tests. Fig. 4 demonstrates that in the presence of both HHF and H_2O_2, the distinctive absorption peaks of these fluoroquinolone antibiotics markedly diminished. This result indicates that the HHF-peroxidase nanozyme has broad-spectrum degradation capability towards fluoroquinolone antibiotics. Notably, when four fluoroquinolone antibiotics were combined, there was a reduction in absorbance, with a degradation efficiency reaching 37% (Fig. S7, ESI†). This suggests the potential application of the HHF-peroxidase nanozyme in treating wastewater containing multiple fluoroquinolone antibiotics.

Since the real water is complex and salt interferences are often present, it is important to examine the interference of

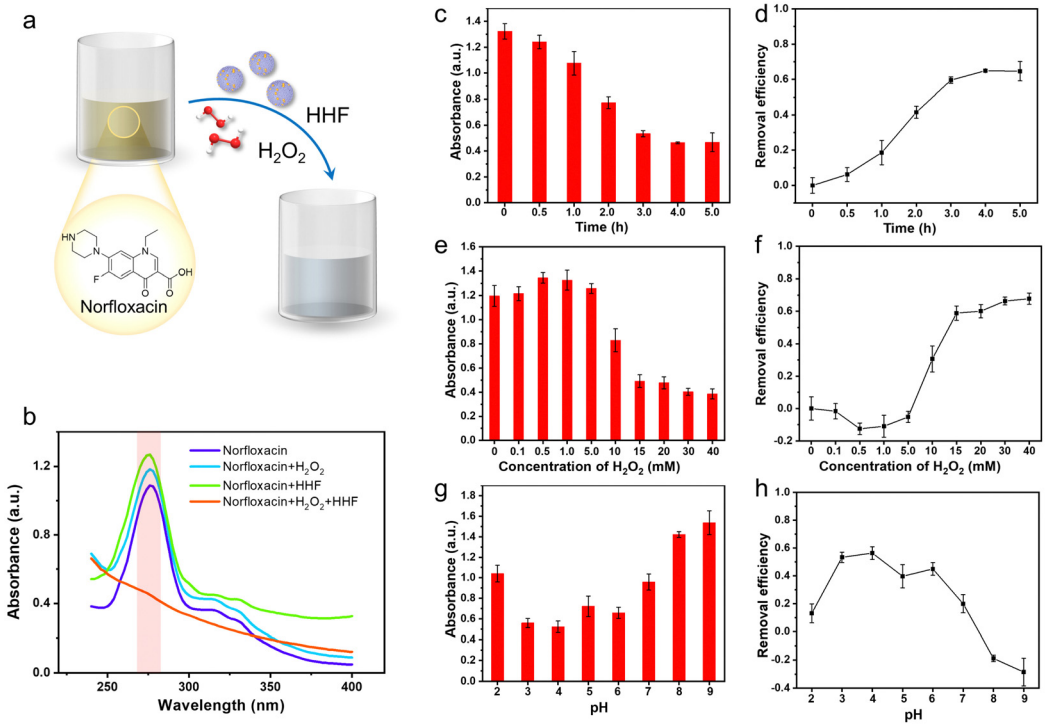

Fig. 3 (a) Schematic illustration of the HHF-peroxidase nanozyme for norfloxacin degradation. (b) UV-vis absorbance spectra of norfloxacin in different reaction systems. (c) and (d) The absorbance and removal efficiency of norfloxacin at different times. (e) and (f) The absorbance and removal efficiency of norfloxacin with different concentrations of H_2O_2. (g) and (h) The absorbance and removal efficiency of norfloxacin at different pH conditions.

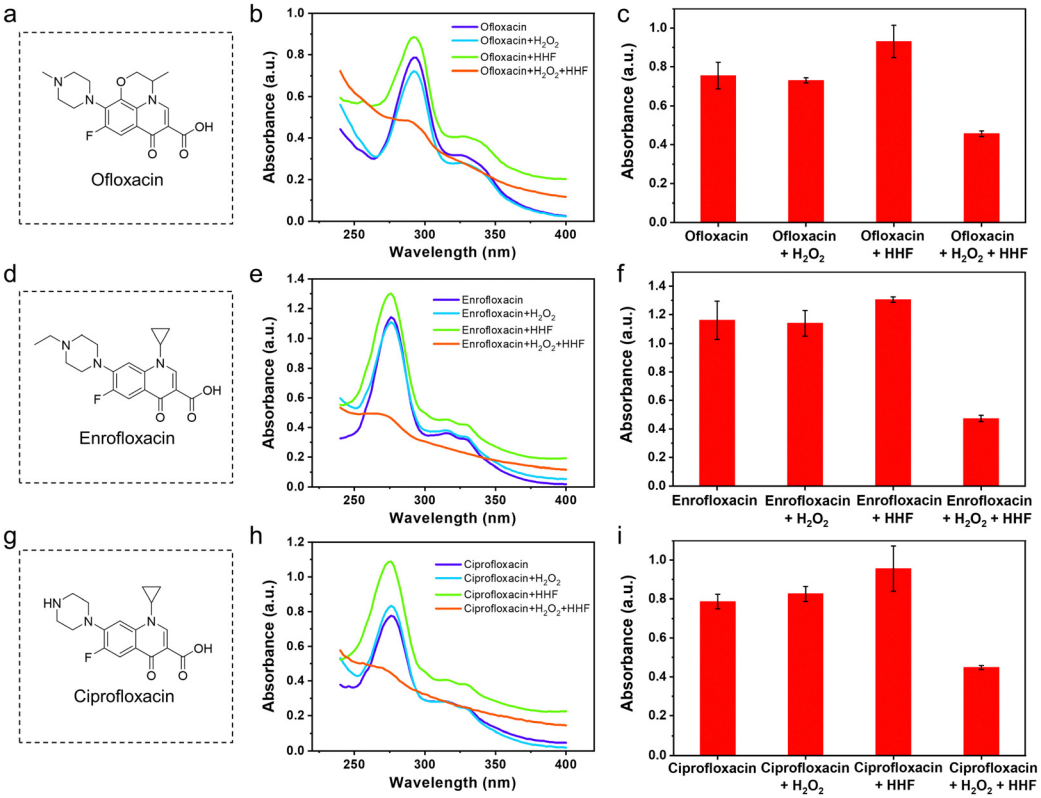

Fig. 4 (a) The structure of ofloxacin. (b) The UV-vis absorbance spectra and (c) absorbance of ofloxacin in different reaction systems. (d) The structure of enrofloxacin. (e) The UV-vis absorbance spectra and (f) absorbance of enrofloxacin in different reaction systems. (g) The structure of ciprofloxacin. (h) The UV-vis absorbance spectra and (i) absorbance of ciprofloxacin in different reaction systems.

different concentrations of salt solutions on the degradation process. Here, NaCl was chosen as an example to carry out the relevant investigation. As shown in Fig. S8 (ESI†), when a series of NaCl (0–10 mM) was present, HHF was still able to perform the catalytic function of peroxidase and the degradation of norfloxacin could be realized. This result indicates that the HHF-peroxidase nanozyme has the potential to achieve antibiotic degradation in complex aqueous environments.

Considering that the HHF-peroxidase nanozyme will be used in aqueous environments, investigating its toxicity is essential. We assessed the cytotoxicity of this nanozyme to HUVEC cells using the CCK-8 assay, which measured cell viability after exposure to various concentrations of the nanozyme. The results, depicted in Fig. S9 (ESI†), show that cell viability remained at 78% when treated with a high concentration of 0.1 mg mL^{-1}. This level of viability suggests that the HHF-peroxidase nanozyme is relatively safe for environmental applications, and can be effectively used in specific concentrations within aqueous settings.

Mechanism of fluoroquinolone antibiotic degradation

The degradation mechanism of fluoroquinolone antibiotics is closely linked to the peroxidase activity of HHF. Firstly, the peroxidase-like activity of HHF was explored under the optimized conditions. As shown in Fig. S10 (ESI†), TMB could be oxidized, as evidenced by a significant absorption peak, indicating that HHF maintains its peroxidase-like activity under the optimal conditions. Peroxidase catalyzes the production of •OH from H_2O_2 with strong oxidizing properties, which is a key factor leading to the degradation of organic molecules.[38] To ascertain •OH production, coumarin was employed as a fluorescence probe due to its unique reactivity with •OH, leading to the emission of intense blue fluorescence around 460 nm.[52] Notably, Fig. 5(a) reveals an amplified fluorescence signal solely in the combined presence of HHF and H_2O_2, confirming •OH's existence. Consequently, it's postulated that •OH is instrumental in the HHF-mediated norfloxacin degradation. Investigating pH influence on •OH formation revealed, as shown in Fig. 5(b), heightened fluorescence intensities under acidic conditions. This pattern aligns with norfloxacin degradation trends, validating the central role of •OH. To consolidate this assertion, isopropanol (IPA), an •OH scavenger, was introduced. Fig. 5(c) and (d) indicate that both the fluorescence of 7-hydroxycoumarin and the degradation magnitude of norfloxacin diminished upon IPA's incorporation, underscoring that the evolved •OH is paramount for norfloxacin degradation.

Degradation of fluoroquinolone antibiotics in real water samples

Fluoroquinolone antibiotics, as evidenced by prior studies, are routinely detected in both lake water and drinking water.[53,54] To investigate the feasibility of the HHF-peroxidase nanozyme

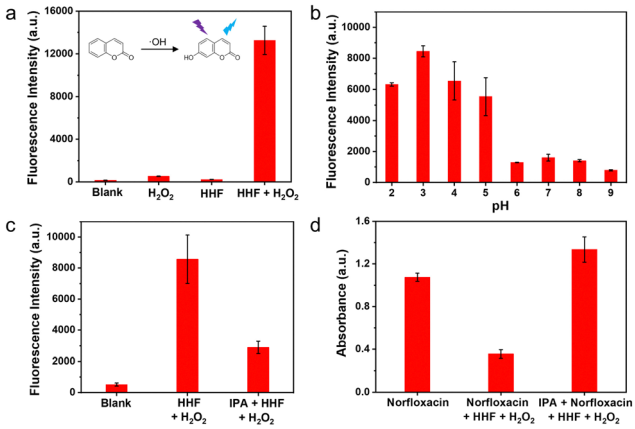

Fig. 5 (a) The fluorescence intensity of 7-hydroxycoumarin in different reaction systems. (b) Hydroxyl radical formation at different pH conditions. (c) The fluorescence intensity of 7-hydroxycoumarin and (d) the absorbance of norfloxacin without or with IPA to scavenge hydroxyl radicals.

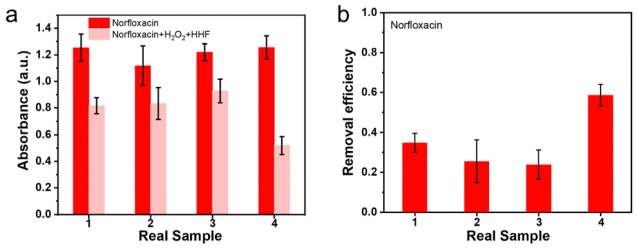

Fig. 6 (a) The absorbance and (b) the removal efficiency of norfloxacin without or with H_2O_2 and the HHF-peroxidase nanozyme in four different real water samples.

to degrade norfloxacin in actual water scenarios, norfloxacin was introduced to four distinct water samples: three from lakes and one from drinking water. Fig. 6(a) and (b) reveal a reduction in norfloxacin absorbance across these samples, though the extent varied. Notably, drinking water exhibited the most significant degradation, with an efficiency reaching 59%. In contrast, the lake waters, which present a more intricate environment, registered removal rates between 24% and 35%. The above results suggest that the HHF-peroxidase nanozyme has the potential to degrade norfloxacin in real water samples. In a parallel examination, three additional fluoroquinolone antibiotics were subjected to degradation tests in real water, and as presented in Fig. S11 (ESI†), the HHF-peroxidase nanozyme successfully degraded all three antibiotics.

Conclusions

The work presented here highlights the promising potential of the HHF-peroxidase nanozyme as an innovative solution for degrading fluoroquinolone antibiotics. Its efficiency is particularly evident in acidic environments when complemented with H_2O_2. Notably, the method has a robust degradation capability for a range of fluoroquinolone antibiotics. Such broad-spectrum capability speaks volumes about the nanozyme's versatility, presenting it as an optimal tool for comprehensive wastewater treatment, especially in settings rife with mixed antibiotic pollutants.

An in-depth examination into the degradation mechanism reveals the integral role of the $^{\bullet}$OH radicals. Furthermore, real-world evaluations, focusing on varied water samples from lakes and drinking sources, attest to the nanozyme's practical relevance. Although the degradation rates varied, reflecting the intricacies of different water environments, the nanozyme consistently demonstrated a commendable antibiotic degradation potential, even in these multifaceted settings.

Given these significant findings, the HHF-peroxidase nanozyme stands out in the battle against the growing challenge of antibiotic pollution in water sources. Its combination of versatility, resilience, and broad-spectrum efficiency earmarks its potential for large-scale wastewater treatments. As we look ahead, it's pertinent to scale up the nanozyme's synthesis and application, gauge its durability, and assess its environmental impact in long-term scenarios. The challenge of antibiotic contamination requires multifaceted approaches, and the development of such efficient nanozymes, as showcased in this research, can be a significant step forward in addressing this global concern.

Author contributions

X. G., X. Y. and B. J. conceptualized and designed the project. X. G., K. S. and Q. H. performed the experiments and analyzed the results. Y. Y. and H. L. provided suggestions on antibiotics model selection. X. G. and B. J. wrote the manuscript.

Data availability

The data supporting this article have been included as part of the ESI.†

Conflicts of interest

There are no conflicts to declare.

Acknowledgements

We acknowledge the financial support from the China Postdoctoral Science Foundation (2022M712873, 2020M682358, 2020TQ0280) and the National Natural Science Foundation of China (no. 32000996).

References

1 Y. Yang, X. Zhang, J. Jiang, J. Han, W. Li, X. Li, K. M. Yee Leung, S. A. Snyder and P. J. J. Alvarez, *Environ. Sci. Technol.*, 2021, **56**, 13–29.
2 K. Fent, A. A. Weston and D. Caminada, *Aquat. Toxicol.*, 2006, **76**, 122–159.
3 M. Patel, R. Kumar, K. Kishor, T. Mlsna, C. U. Pittman Jr. and D. Mohan, *Chem. Rev.*, 2019, **119**, 3510–3673.

4 T. D. M. Pham, Z. M. Ziora and M. A. T. Blaskovich, *MedChemComm*, 2019, **10**, 1719–1739.
5 A. M. Emmerson and A. M. Jones, *J. Antimicrob. Chemother.*, 2003, **51**, 13–20.
6 L. A. Mitscher, *Chem. Rev.*, 2005, **105**, 559–592.
7 Q.-Q. Zhang, G.-G. Ying, C.-G. Pan, Y.-S. Liu and J.-L. Zhao, *Environ. Sci. Technol.*, 2015, **49**, 6772–6782.
8 L. S. Redgrave, S. B. Sutton, M. A. Webber and L. J. V. Piddock, *Trends Microbiol.*, 2014, **22**, 438–445.
9 K. J. Aldred, R. J. Kerns and N. Osheroff, *Biochemistry*, 2014, **53**, 1565–1574.
10 T. Paul, P. L. Miller and T. J. Strathmann, *Environ. Sci. Technol.*, 2007, **41**, 4720–4727.
11 Y. Gou, P. Chen, L. Yang, S. Li, L. Peng, S. Song and Y. Xu, *Chemosphere*, 2021, **270**, 129481.
12 M. J. Ahmed, *Environ. Toxicol. Pharmacol.*, 2017, **50**, 1–10.
13 M. Zou, W. Tian, J. Zhao, M. Chu and T. Song, *Process Saf. Environ. Prot.*, 2022, **160**, 116–129.
14 H. Fu, X. Li, J. Wang, P. Lin, C. Chen, X. Zhang and I. H. M. Suffet, *J. Environ. Sci.*, 2017, **56**, 145–152.
15 E. A. Serna-Galvis, J. Silva-Agredo, A. M. Botero-Coy, A. Moncayo-Lasso, F. Hernández and R. A. Torres-Palma, *Sci. Total Environ.*, 2019, **670**, 623–632.
16 X. Chen, R. Zhuan and J. Wang, *J. Hazard. Mater.*, 2021, **404**, 124172.
17 X. Lv, D. Y. S. Yan, F. L.-Y. Lam, Y. H. Ng, S. Yin and A. K. An, *Chem. Eng. J.*, 2020, **401**, 126012.
18 M. Sayed, A. Arooj, N. S. Shah, J. A. Khan, L. A. Shah, F. Rehman, H. Arandiyan, A. M. Khan and A. R. Khan, *J. Mol. Liq.*, 2018, **272**, 403–412.
19 H. Yu, G. Liu, L. Shen, R. Jin, J. Zhou, H. Guo and L. Wang, *J. Hazard. Mater.*, 2023, **444**, 130394.
20 S. Man, H. Bao, K. Xu, H. Yang, Q. Sun, L. Xu, W. Yang, Z. Mo and X. Li, *Chem. Eng. J.*, 2021, **417**, 129266.
21 Y. Chen, F. Li, X. Dong, D. Guo, Y. Huang and S. Li, *J. Alloys Compd.*, 2021, **869**, 159258.
22 S.-B. Hu, L. Li, M.-Y. Luo, Y.-F. Yun and C.-T. Chang, *Ultrason. Sonochem.*, 2017, **38**, 446–454.
23 X. Ma, Y. Cheng, Y. Ge, H. Wu, Q. Li, N. Gao and J. Deng, *Ultrason. Sonochem.*, 2018, **40**, 763–772.
24 G. Yang, Y. Liang, J. Yang, X. Zhang, Z. Zeng, Z. Xiong, J. Jia and K. Sa, *J. Environ. Chem. Eng.*, 2023, **11**, 109328.
25 C. Geng, Z. Liang, F. Cui, Z. Zhao, C. Yuan, J. Du and C. Wang, *Chem. Eng. J.*, 2020, **383**, 123145.
26 L. Gao, J. Zhuang, L. Nie, J. Zhang, Y. Zhang, N. Gu, T. Wang, J. Feng, D. Yang, S. Perrett and X. Yan, *Nat. Nanotechnol.*, 2007, **2**, 577–583.
27 H. Wei and E. Wang, *Chem. Soc. Rev.*, 2013, **42**, 6060–6093.
28 H. Ding, B. Hu, B. Zhang, H. Zhang, X. Yan, G. Nie and M. Liang, *Nano Res.*, 2021, **14**, 570–583.
29 A. A. Vernekar, D. Sinha, S. Srivastava, P. U. Paramasivam, P. D'Silva and G. Mugesh, *Nat. Commun.*, 2014, **5**, 5301.
30 J. Wu, X. Wang, Q. Wang, Z. Lou, S. Li, Y. Zhu, L. Qin and H. Wei, *Chem. Soc. Rev.*, 2019, **48**, 1004–1076.
31 Y. Huang, J. Ren and X. Qu, *Chem. Rev.*, 2019, **119**, 4357–4412.
32 H. Wang, K. Wan and X. Shi, *Adv. Mater.*, 2019, **31**, 1805368.
33 M. Liang and X. Yan, *Acc. Chem. Res.*, 2019, **52**, 2190–2200.
34 Z. Wang, R. Zhang, X. Yan and K. Fan, *Mater. Today*, 2020, **41**, 81–119.
35 F. Liu, L. Lin, Y. Zhang, Y. Wang, S. Sheng, C. Xu, H. Tian and X. Chen, *Adv. Mater.*, 2019, **31**, 1902885.
36 J. Fang, H. Wang, X. Bao, Y. Ni, Y. Teng, J. Liu, X. Sun, Y. Sun, H. Li and Y. Zhou, *Carbon*, 2020, **169**, 370–381.
37 J. Zhang, J. Zhuang, L. Gao, Y. Zhang, N. Gu, J. Feng, D. Yang, J. Zhu and X. Yan, *Chemosphere*, 2008, **73**, 1524–1528.
38 S. Zhang, X. Zhao, H. Niu, Y. Shi, Y. Cai and G. Jiang, *J. Hazard. Mater.*, 2009, **167**, 560–566.
39 Y. Ding, Z. Li, W. Jiang, B. Yuan, T. Huang, L. Wang and J. Tang, *Catal. Commun.*, 2020, **134**, 105859.
40 Z. Zhang, J. Hao, W. Yang, B. Lu, X. Ke, B. Zhang and J. Tang, *ACS Appl. Mater. Interfaces*, 2013, **5**, 3809–3815.
41 A. Zeb, X. Xie, A. B. Yousaf, M. Imran, T. Wen, Z. Wang, H.-L. Guo, Y.-F. Jiang, I. A. Qazi and A.-W. Xu, *ACS Appl. Mater. Interfaces*, 2016, **8**, 30126–30132.
42 P. K. Boruah and M. R. Das, *J. Hazard. Mater.*, 2020, **385**, 121516.
43 X. Bian, D. Chen and L. Han, *Chem. Eng. J.*, 2022, **429**, 132317.
44 M. Zandieh and J. Liu, *Angew. Chem., Int. Ed.*, 2022, **61**, e202212013.
45 X. Zhao, T. Yang, D. Wang, N. Zhang, H. Yang, X. Jing, R. Niu, Z. Yang, Y. Xie and L. Meng, *Anal. Chem.*, 2022, **94**, 4484–4494.
46 S. Wu, W. Wu, Z. Zhu, M. Li, J. Zhao and S. Dong, *Nano Res.*, 2023, **16**, 10840–10847.
47 K. Fan, H. Wang, J. Xi, Q. Liu, X. Meng, D. Duan, L. Gao and X. Yan, *Chem. Commun.*, 2017, **53**, 424–427.
48 S. Liang, X.-L. Wu, M.-H. Zong and W.-Y. Lou, *J. Colloid Interface Sci.*, 2022, **622**, 860–870.
49 J. Chen, L. Huang, Q. Wang, W. Wu, H. Zhang, Y. Fang and S. Dong, *Nanoscale*, 2019, **11**, 5960–5966.
50 N. C. Veitch, *Phytochemistry*, 2004, **65**, 249–259.
51 E. Derat and S. Shaik, *J. Phys. Chem. B*, 2006, **110**, 10526–10533.
52 K.-i Ishibashi, A. Fujishima, T. Watanabe and K. Hashimoto, *Electrochem. Commun.*, 2000, **2**, 207–210.
53 X. Liu, S. Lu, W. Guo, B. Xi and W. Wang, *Sci. Total Environ.*, 2018, **627**, 1195–1208.
54 R. Zhao, X. Li, M. Hu, S. Li, Q. Zhai and Y. Jiang, *Bioprocess Biosyst. Eng.*, 2017, **40**, 1261–1270.

